frontiers in Environmental Science

ORIGINAL RESEARCH
published: 02 March 2022
doi: 10.3389/fenvs.2022.816361

Effects of *In Situ* Remediation on Copper Distribution and Soil Aggregate Adsorption–Desorption Characteristics in Smelter-Impacted Soil

Lei Xu[1,2]*, *Xiangyu Xing*[3], *Jianbiao Peng*[4] *and Mingfei Ji*[2]*

[1]Key Laboratory of Natural Disaster and Remote Sensing of Henan Province, Nanyang Normal University, NanYang, China, [2]Henan Key Laboratory of Ecological Security for Water Source Region of Mid-line of South-to-North Diversion Project, NanYang, China, [3]College of Non-Major Foreign Language Teaching, Nanyang Normal University, Nanyang, China, [4]School of Environment, Henan Normal University, Xinxiang, China

OPEN ACCESS

Edited by:
Nabeel Khan Niazi,
University of Agriculture Faisalabad, Pakistan

Reviewed by:
Andrew Hursthouse,
University of the West of Scotland, United Kingdom
Yu Shi,
Institute of Soil Science (CAS), China

***Correspondence:**
Lei Xu
hedaxl@163.com
Mingfei Ji
jimfdy@gmail.com

Specialty section:
This article was submitted to Toxicology, Pollution and the Environment, a section of the journal Frontiers in Environmental Science

Received: 16 November 2021
Accepted: 09 February 2022
Published: 02 March 2022

Citation:
Xu L, Xing X, Peng J and Ji M (2022) Effects of In Situ Remediation on Copper Distribution and Soil Aggregate Adsorption–Desorption Characteristics in Smelter-Impacted Soil. Front. Environ. Sci. 10:816361. doi: 10.3389/fenvs.2022.816361

To evaluate the effect of *in situ* chemical remediation on copper (Cu) immobilisation and migration, *in situ* chemically remediated soils from a smelter-impacted field were partitioned into four aggregate size fractions and their Cu adsorption characteristics were investigated. The results indicate that the highest Cu concentration occurred in the <0.053 mm size fraction, while the highest Cu mass loading was obtained in the 0.25–2 mm size fraction (39.9–42.5%). However, *in situ* remediation increased the Cu mass loading levels in the >0.25 mm aggregates. A pseudo-second-order model was used to fit the adsorption process obtained in kinetic experiments, while the data from isothermal experiments were described using the Freundlich model. The fastest adsorption rate was observed in the <0.053 mm fraction, and the adsorption capacity of the soil aggregates improved after combined *in situ* remediation. The amount of Cu^{2+} adsorbed increased with increasing pH. The <0.053 mm fraction exhibited lower desorption compared with the other fractions at low pH values. In addition, all particle size aggregates treated with apatite and *Elsholtzia splendens* had the lowest desorption rates at different pH values.

Keywords: smelter-impacted soil, *in situ* remediation, soil aggregate, isothermal adsorption, desorption

1 INTRODUCTION

Due to rapid industrial and agricultural development, heavy metals can enter the soil in large quantities through agricultural activity, atmospheric sedimentation, and wastewater irrigation, among others. Heavy metals that accumulate in the soil not only reduce the soil quality, its microbial activity, and crop yields, but also threaten ecosystem security and human health (Zhang et al., 2015). In recent decades, researchers have conducted a variety of studies to develop practices that solve the problem of soil heavy metal pollution, including bioremediation and integrated remediation. However, some technologies are not suitable for practical applications owing to their limitations. The combined use of plant-based and chemical additives for *in situ* remediation is one of the most inexpensive and effective methods for remediating soils contaminated by heavy metals (Xu et al., 2020; Li et al., 2021). Chemical remediation mainly involves the addition of low toxicity or

TABLE 1 | Physical and chemical properties of the soil in the study area.

pH	CEC	SOC	TN	TP	TK	An	EP	AK	T-Cu	$CaCl_2$-Cu
	cmol kg^{-1}	g kg^{-1}	g kg^{-1}	g kg^{-1}	g kg^{-1}	mg kg^{-1}	mg kg^{-1}	mg kg^{-1}	mg kg^{-1}	mg kg^{-1}
4.63	8.45	16.3	1.33	0.261	2.38	67.1	186	54.8	517	48.7

non-toxic inorganic chemical materials to the soil, which can change the heavy metal mobility in the soil by changing the soil properties and environment (Jin and Kwak, 2019). Inorganic chemical materials including lime, apatite, zeolite, iron manganese oxide, silicate, sepiolite, red mud, bone char, compost, steel slag, montmorillonite, attapulgite, and vermiculite have been reported to effectively stabilise heavy metals in soil and reduce the bioavailability of heavy metals (Zheng et al., 2012). In addition, previous research has shown that potential metal mobility in the soil is mainly determined by the adsorption–desorption process (Samsuri et al., 2019). Through adsorption, heavy metals only accumulate in the topsoil in the case of relatively low concentrations; however, they will migrate to the deeper soil layers and can contaminate groundwater by rainwater leaching or irrigation when the pollution exceeds a certain level (Haynes and Graham, 2004). Metals retained in the topsoil are not only a potential hazard to plants, animals, and microorganisms, but also pose major threats to human health through the food chain (He et al., 2020).

As the basic unit of soil structure, the study of aggregate forms, stability, and its influencing factors is critical for maintaining good soil structure and fertility, as well as for reducing pollutant migration (Zhao et al., 2017). Due to different physical and chemical characteristics, the abilities of various particle size aggregates to adsorb foreign materials (metals, N, P, etc.) may differ, and it is generally accepted that fine soil particles have a higher capacity to carry heavy metals than coarser particles, owing to their larger specific surface area and higher organic matter and Fe/Mn/Al oxide contents (Xu et al., 2013a; Xiao et al., 2016; Huang et al., 2017; Xu et al., 2017). Further, the fine soil fractions are often preferentially transported into the deep soil, surface/groundwater, and air (Nejad et al., 2021). Therefore, it is necessary to study the adsorption process between heavy metals and soil aggregates in different size fractions to determine the associated environmental risks during remediation. To date, although some related studies have been conducted (Huang et al., 2020), most of the previous studies have been conducted using urban soil (Li et al., 2015), dust (Ma and Singhirunnusorn, 2012), and sediment (Yu et al., 2011), while arable soil has not been investigated. In addition, the distribution of the aggregates and the changes in the adsorption characteristics of heavy metal ions to the aggregates during the remediation process have not been evaluated.

In southern China, excess heavy metals in the soil are becoming increasingly serious due to industrial and agricultural activity. Due to the low soil pH, as well as the high activity and toxicity of the heavy metals in the soil, agricultural production in this region has been seriously impacted (Xue et al., 2012; Zhu et al., 2018); therefore, it is important to investigate soil heavy metal remediation in this region and determine the effects of remediation on the metal adsorption–desorption with soil aggregates, which is critical for evaluating the remediation effects and environmental risks after remediation (Alireza and Fahadani, 2018; Zhang et al., 2020). In this study, the effects of three types of inorganic chemical materials (soda residue, apatite, and lime) on Cu availability and distribution in bulk soil were investigated. We also explored the effects of combined remediation approaches on Cu distribution in soil aggregates, and kinetic, isothermal adsorption, and pH experiments were used to determine the adsorption–desorption characteristics of Cu onto various soil aggregates. This study provides new insights into the adsorption mechanism between soil aggregates and heavy metals, and assesses the heavy metal pollution risk in the soil during remediation.

2 MATERIALS AND METHODS

2.1 Experimental Design

The experimental site was located in Guixi City, Jiangxi Province, China. The residents in this area use Cu-contaminated water that is discharged from a copper smelter for farmland irrigation and atmospheric metal deposition, resulting in heavy metal pollution (mainly Cu) on more than 130 hm^2 of the surrounding farmland (Li et al., 2009). To reduce the soil pollution hazards in this area, field experiments were conducted in triplicate and were designed using a randomised block. Each plot covered 6 m^2 (3 m × 2 m) and was separated by plastic plates. Four remediation treatments were applied: 1) 0.5% soda residue (w/w according to the mass of the upper 0.17 m of soil, 2) 1% apatite, 3) 0.2% lime, and 4) no remediation (control). The material doses used in the experiment were based on previous research results (Xu et al., 2017). The materials were added to the soil on 26 December 2012 and were mixed fully with the soil using a rotary cultivator. *Elsholtzia splendens* were planted on 26 April 2013 2014, and 2015, with a planting density of 0.3 m × 0.3 m. A compound fertiliser was applied before the plants were planted at a rate of 0.833 t ha^{-1}. During 2012–2015, remediation materials were applied only in 2012, and the *Elsholtzia splendens* were harvested in mid-December of each year. All plots were managed using the same field management. Weeds were cleared from all plots before planting every year, and no weeding was carried out thereafter.

TABLE 2 | Soil properties after 3 years of remediation.

Treatment	pH	SOC	TN	TP	TK	AN	EP	AK	T-Cu	$CaCl_2$-Cu
		g kg^{-1}	g kg^{-1}	g kg^{-1}	g kg^{-1}	Mg kg^{-1}	mg kg^{-1}	mg kg^{-1}	mg kg^{-1}	mg kg^{-1}
CK	4.59 ± 0.299b	16.4 ± 0.132b	1.34 ± 0.134a	0.263 ± 0.0321b	2.38 ± 0.362a	33.5 ± 2.03b	93.4 ± 6.12b	60.9 ± 10.7c	517 ± 61.7a	48.7 ± 5.35a
AS	5.27 ± 0.208a	21.8 ± 0.303a	1.47 ± 0.0103a	0.210 ± 0.0100b	2.29 ± 0.208a	48.8 ± 2.17a	144 ± 7.02a	96.5 ± 6.63a	561 ± 69.0a	36.0 ± 6.88 ab
AP	5.49 ± 0.0551a	18.6 ± 0.152ab	1.37 ± 0.218a	0.400 ± 0.0265a	2.42 ± 0.0473a	45.5 ± 2.36a	152 ± 13.6a	84.7 ± 6.33ab	592 ± 55.1a	14.1 ± 4.43c
LI	5.27 ± 0.351a	18.0 ± 0.174ab	1.57 ± 0.153a	0.210 ± 0.0100b	2.51 ± 0.206a	48.7 ± 1.22a	153 ± 4.08a	75.2 ± 7.18bc	554 ± 43.0a	31.5 ± 6.27b

2.2 Soil and Amendments

Soil was collected and its properties were analysed before remediation. The soil properties are listed in **Table 1**. After the field immobilisation, remediation was performed for 3 years. Soil samples were collected from each plot, with volumes of 0.20 m × 0.2 m × 0.17 m, and three samples were selected and mixed to form a representative sample from each plot. These samples were air-dried and sieved through a 5 mm sieve for soil aggregate analysis. The surface soil (0—0.17 m) was also collected and passed through a 2 mm sieve to determine its basic properties and Cu concentration.

The Cu concentrations of soda residue (0.25 mm particle size, Sinopec Group Lianyungang Soda Plant, Jiangsu, China), apatite (0.25 mm particle size, Nan Zhang Chang Bai Mineralization Industry Co., Ltd., Hubei, China), and lime (0.25 mm particle size, building materials market, Jiangxi, China) were 0.412 mg kg^{-1}, 9.54 mg kg^{-1}, and 1.36 mg kg^{-1}, respectively. The pH values of the soda residue, apatite, and lime were 10.1, 8.40, and 12.2, respectively.

2.3 Adsorption and Desorption Experiments

Adsorption experiments were conducted to evaluate the Cu^{2+} adsorption capacity of the soil aggregates after remediation. The adsorption isotherms, initial pH, and adsorption kinetics were evaluated using a guaranteed reagent. A copper standard solution was used to prepare the Cu^{2+} solutions, and 0.1 mol L^{-1} HNO_3 and NaOH were used to adjust the solution pH.

2.3.1 Isothermal Adsorption

Aggregates (0.5 g) of different particle sizes were placed into a 50 ml polypropylene centrifuge tube, and 25 ml of Cu^{2+} solution with various concentrations (10, 20, 50, 100, and 200 mg L^{-1}) were added. The suspensions were shaken at 160 rpm for 4.0 h and then kept still for 20.0 h at a constant temperature of 25 ± 0.2°C. The samples were then centrifuged at 4,000 rpm for 20 min and the supernatants were filtrated through a 0.45 μm micro membrane for analysis of the Cu^{2+} concentrations. To analyse the adsorption characteristics of Cu^{2+} by the aggregates, the Langmuir and Freundlich equations were used to simulate the adsorption (**Eqs 1**, **2**, respectively):

$$q_e = \frac{K_L q_L C_e}{1+K_L C_e} \quad (1)$$

$$q_e = K_F C_e^{\frac{1}{n}} \quad (2)$$

where q_e is the equilibrium adsorption capacity (mg kg^{-1}), C_e is the Cu^{2+} concentration of the solution when the adsorption reaches equilibrium (mg L^{-1}), q_L is the maximum Cu^{2+} adsorption capacity of the aggregate (mg kg^{-1}), and K_L (L mg^{-1}), K_F (L mg^{-1}), and *1/n* are constants.

2.3.2 Kinetic Adsorption

Analysis of the kinetic process is helpful for understanding the adsorbent's adsorption rate for metal ions in solution. The kinetic experiments were conducted according to the following steps. Aggregates (1 g) of different size fractions were added to the

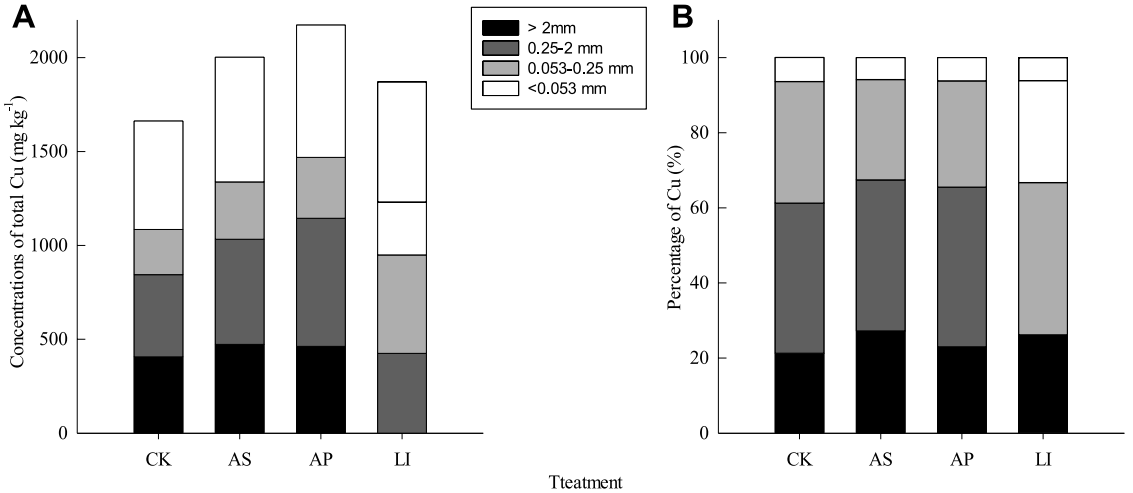

FIGURE 1 | (A) Total Cu concentrations for different soil aggregate size fractions and treatments. **(B)** Total Cu mass loading values for different soil aggregate size fractions and treatments. CK = untreated soil, AS = soda residue + *Elsholtzia splendens*, AP = apatite + *Elsholtzia splendens*, LI = lime + *Elsholtzia splendens*.

aqueous solution (100 mg L^{-1}, pH 5, 50 ml) and shaken at 160 rpm at 30°C for 4 h in a reciprocating shaker. Samples (5 ml) were collected using a pipette (Eppendorf, Research Plus, 0.5–5 ml) after 5, 10, 20, 30, 60, 120, 240, and 480 min. After equilibration, the suspensions were centrifuged at 4,000 rpm for 20 min, and the supernatant was filtered though a 0.45 μm micro membrane to determine the Cu^{2+} concentrations.

To analyse the adsorption kinetics, pseudo-first-order (Mobasherpour et al., 2014) and pseudo-second-order kinetic (Ho and McKay, 2000) equations were used to fit the adsorption data (**Eqs 3**, **4**, respectively):

$$\ln(Q_e - Q_t) = \ln Q_e - k_1 t \quad (3)$$

$$t/Q_t = 1/k_2 Qe^2 + t/Q_e \quad (4)$$

where k_1 (min^{-1}) and k_2 (g mg^{-1} min^{-1}) are the adsorption rate constants, and Q_e and Q_t (mg g^{-1}) are the amounts of solute adsorbed per unit of adsorbent at equilibrium and at time t, respectively. The initial adsorption rate v_0 (mg g^{-1} min^{-1}) was calculated using $v_0 = k_2 Q_e^2$.

2.3.3 Adsorption and Desorption at Different pH Values

In order to understand the effect of pH on Cu^{2+} adsorption and desorption by the soil aggregates, 0.5 g of aggregates in different size fraction were placed into a 50 ml polypropylene centrifuge tube, to which 25 ml of Cu^{2+} solution with pH values of 2.0, 3.5, 5.0, and 6.5 were added. The method and measurement of Cu^{2+} were the same as those used in the isotherm adsorption experiments. Then, 25 ml of 0.01 mol L^{-1} $NaNO_3$ was added to each tube to replace the Cu^{2+} and the following methods (shaking, equilibration, centrifugation, and separation) were the same as those used the isotherm adsorption experiments. The total desorption capacity of Cu^{2+} was obtained by repeating these operations three times.

2.4 Chemical Analyses

Soil pH was measured using a glass electrode at a water:soil ratio of 2.5:1 (PHS-2CW-CN, Bante, Shanghai, China). Soil organic carbon (SOC) and total nitrogen were determined according to the Deshpande's method (Deshpande et al., 1958). Soil available phosphate (P) and nitrogen (N) were measured according to Bingham's method (Page, 1992). The CEC was measured using the ammonium acetate method (Pansu and Gautheyrou, 2006). The total Cu in the bulk soil and aggregate size fractions, and the available Cu in the bulk soil were measured according to the methods of Pansu (Pansu and Gautheyrou, 2006).

2.5 Aggregate Analyses

The soil aggregates were divided into >2 mm, 0.25–2 mm, 0.053–0.25 mm, and <0.053 mm according to Elliott's method (Shaver et al., 2003).

2.6 Statistical Analyses

All treatments were performed in triplicate. All of the data used in this study were analysed using the SPSS 20.0 software package and Excel 2010 (Microsoft, USA). Sigmaplot 12.5 was used to generate the graphics.

3 RESULTS AND DISCUSSION

3.1 Soil Characteristics and Plant Biomass

After 3 years of *in situ* remediation using soda residue, apatite, and lime on Cu-contaminated soil that contained *Elsholtzia splendens*, the soil pH increased, while the available Cu decreased significantly (**Table 2**). After 3 years of remediation, the SOC contents increased owing to the application of these three amendments. The highest SOC contents were observed in the soda residue treatment group, followed by the apatite and lime treatment groups. Plant growth might be achieved by increasing the amount of litter and fine roots, and by changing the structures of soil aggregates, which further leads

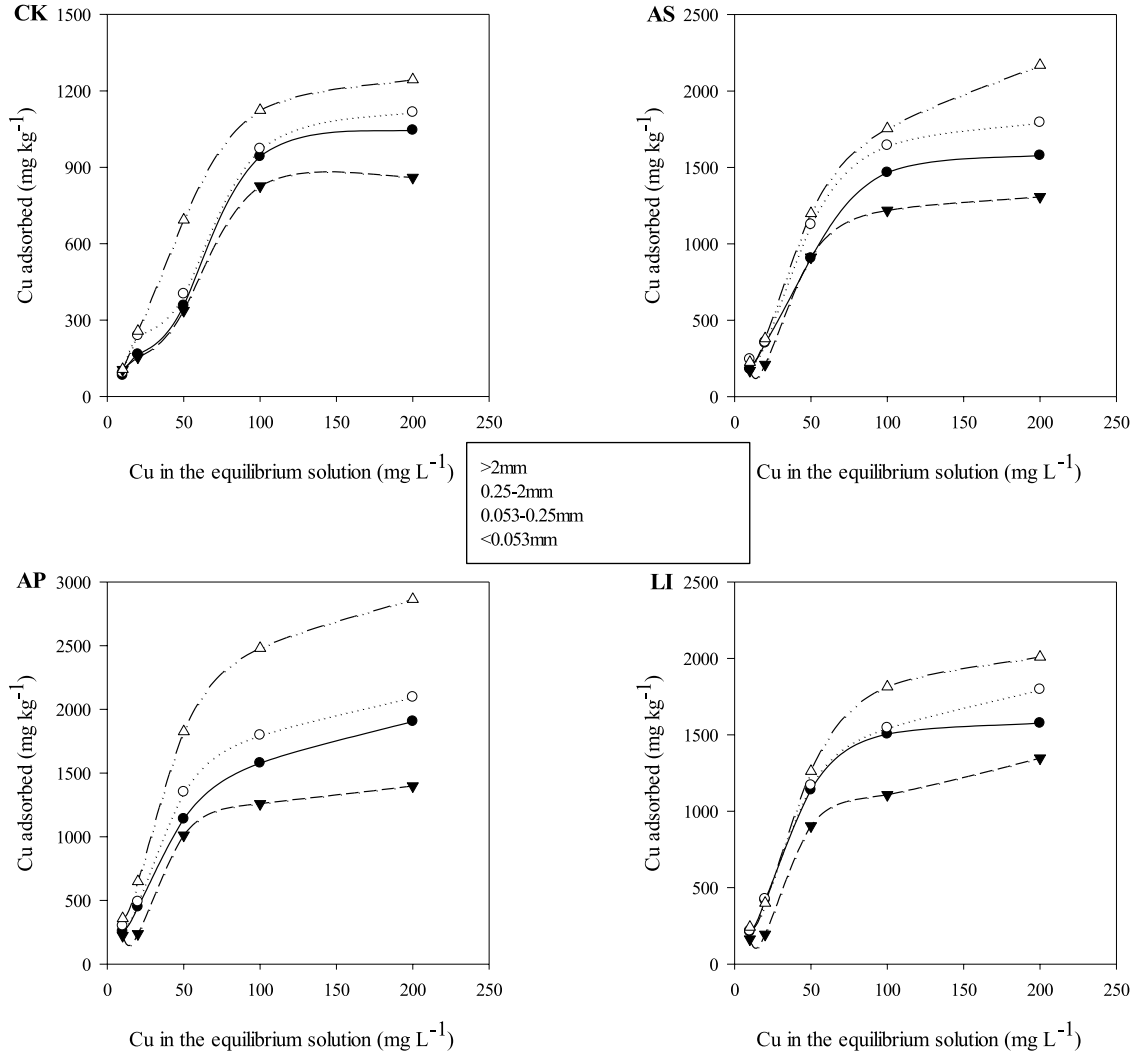

FIGURE 2 | Adsorption isotherms for Cu onto the soil aggregates. CK = untreated soil, AS = soda residue + *Elsholtzia splendens*, AP = apatite + *Elsholtzia splendens*, LI = lime + *Elsholtzia splendens*.

to increases in SOC content (Pez-Bellido et al., 2010; Li et al., 2017). The remediation materials combined with planting *Elsholtzia splendens* did not have a major effect on soil total N or total K; however, the application of apatite could improve the total phosphorus concentration in the soil. This may be because apatite contains large amounts of phosphorus, which dissolves after being applied to the soil. In addition, this region typically experiences acid rain settling (Tao et al., 2014), which may facilitate apatite dissolution (Oliva et al., 2012; Brahim et al., 2017), thereby increasing the soil total and available phosphorus concentrations. The total Cu concentration increased slightly in the remediated soils that received a combined treatment (**Table 2**). This was mainly because of severe atmospheric deposition that occurs in this area, whereby heavy metals continually enter the soil, while surface runoff and leaching amounts varied widely among the different treatments (Madej et al., 2010; Yao et al., 2018). This could lead to an increased Cu adsorption and retention capacity, which has resulted in a slight increase in the total Cu concentration in the remediation soil (Cui et al., 2016).

(SOC = soil organic carbon, TN = soil total nitrogen, TP = soil total phosphorus, AN = soil available nitrogen, EP = soil effective phosphorus, AK = soil available potassium, T-Cu = soil total Cu, CK = untreated soil, AS = soda residue + *Elsholtzia splendens*, AP = apatite + *Elsholtzia splendens*, LI = lime + *Elsholtzia splendens*. Different lowercase letters indicate significant differences between treatments during the same year, $n = 3$, $p < 0.05$).

3.2 Cu and Cd Contents in the Wet Aggregate Fractions

Wet aggregates have been used to study changes in heavy metal distributions during long-term soil use (Hardie et al., 2014). Thus, we measured the Cu concentrations and distributions in wet aggregates. The highest Cu concentration was observed in the

TABLE 3 | Langmuir and Freundlich model parameters and R-squared values calculated from Cu isotherm experimental data.

Treatment	Particle size (mm)	Langmuir			Freundlich		
		KL (L mg-1)	qL (mg kg-1)	R2	KF (L mg-1)	n	R2
CK	>2	0.00425	2.60 × 103	0.637	0.0140	1.14	0.960
	0.25–2	0.00661	2.17 × 103	0.767	0.0213	1.24	0.946
	0.053–0.25	0.00825	1.50 × 103	0.808	0.0218	1.35	0.949
	<0.053	0.00945	2.14 × 103	0.807	0.0270	1.24	0.916
AS	>2	0.0170	2.23 × 103	0.944	0.0600	1.43	0.924
	0.25–2	0.0216	2.38 × 103	0.931	0.0924	1.57	0.894
	0.053–0.25	0.0133	1.98 × 103	0.765	0.0459	1.41	0.843
	<0.053	0.0148	3.21 × 103	0.914	0.0755	1.39	0.916
AP	>2	0.0256	2.39 × 103	0.989	0.115	1.68	0.936
	0.25–2	0.0332	2.53 × 103	0.983	0.156	1.78	0.907
	0.053–0.25	0.0178	1.92 × 103	0.819	0.0738	1.62	0.814
	<0.053	0.0489	3.31 × 103	0.987	0.262	1.86	0.857
LI	>2	0.0286	1.97 × 103	0.963	0.103	1.67	0.886
	0.25–2	0.0230	2.33 × 103	0.966	0.0914	1.56	0.892
	0.053–0.25	0.0106	2.18 × 103	0.700	0.0408	1.38	0.846
	<0.053	0.0212	2.70 × 103	0.931	0.0942	1.51	0.885

CK = untreated soil, AS = soda residue + Elsholtzia splendens, *AP = apatite* + Elsholtzia splendens, *LI = lime* + Elsholtzia splendens.

<0.053 mm size fraction, followed by the 0.25–2 mm, > 2 mm, and 0.053–0.25 mm size fractions (**Figure 1A**) The Cu concentrations in both the >2 mm and 0.25–2 mm size fractions followed the order of soda residue > apatite > lime > control, while the Cu concentrations in both the 0.053–0.25 mm and <0.053 mm size fractions followed a descending order of apatite > soda residue > lime > control. The highest Cu mass loading was observed in the 0.25–2 mm size fraction (39.9–42.5%), followed by the 0.053–0.25 mm (26.7–32.4%), >2 mm (21.3–27.2%), and <0.053 mm (5.85–6.37%) size fractions (**Figure 1B**).

Similar to the results of our previous study (Xu et al., 2013b), the highest heavy metal concentrations were observed in the <0.053 mm aggregates, which might be due to their larger surface areas. Thus, heavy metals can easily accumulate on these large surface areas by adsorption, forming chelating complexes with colloidal organic mineral particles in the finest fractions (Lo et al., 2016). In addition, only 2.9–18.3% heavy metal loading was observed in the <0.053 mm size fraction, while the >2 mm and 0.25–2 mm size fractions were important Cu reservoirs in all of the soils, which may be due to the higher aggregate contents of the >2 mm and 0.25–2 mm size fractions. Notably, after remediation, the mass loading capacities of Cu in the >2 mm and 0.25–2 mm size fractions were promoted.

3.3 Adsorption Isotherms

Figure 2 shows the experimental data and adsorption isotherms for Cu adsorption onto the soil aggregates. From the fitting results, when the initial copper ion concentration is low, the adsorption capacity of the aggregates for copper ions increased rapidly with an increase in copper ion concentrations. However, when the copper ion concentration in the solution exceeded 100 mg L^{-1}, the growth of aggregates for copper ions was gentle, as was the increase in copper ion concentration. Significant differences were observed among the adsorption capacities of the different particle size aggregates for Cu, with the adsorption capacity of the 0.053 mm size fraction as the strongest among all four particle sizes, followed by 0.25–2 mm, > 2 mm, and 0.053–0.25 mm. In addition, we found that the maximum adsorption capacity of each aggregate particle size for Cu was improved after combined remediation, with increases of 50.8–82.3%, 60.7–87.8%, 52.2–62.6%, and 61.5–130% in the >2 mm, 0.25–2 mm, 0.053–0.25 mm, and <0.053 mm aggregates, respectively. The AP treatment exhibited the largest improvement in the adsorption capacity of the aggregates among all the treatments, while AS and LI had similar ranges of increase. The adsorption capacity of the soil that underwent combined remediation increased compared to that of CK, which may be due to the higher organic matter content. Recent studies have shown that organic matter can affect metal contents negatively or positively, owing to the formation of metal chelates or complexes, and the binding of the metal cations to organic matter can control the concentrations and toxicity of free metal ions in the soil solution (Mariela and Fernandez, 2015). Based on this theory, the lower organic matter content of the CK soil led to a lower Cu adsorption rate than in the soil that underwent combined remediation.

The Langmuir and Freundlich isotherm parameters are presented in **Table 3**. The R^2 values for the Langmuir and Freundlich isotherms ranged from 0.637 to 0.989 and from 0.814 to 0.960, respectively, for Cu. From the R^2 values of the two fitted models, the fitting accuracy of the Freundlich model was better than that of the Langmuir model. As presented in **Table 3**, the maximum Cu adsorption capacity (q_L, calculated from the Langmuir equation) was 1.50×10^3–3.31×10^3 mg kg^{-1}. In addition, we found that the q_L of the <0.053 mm size fraction was the largest, except for the CK treatment, while the q_L value of the <0.053 mm size fraction was 1.16–1.72 times those of the other size fractions. This indicates that the <0.053 mm aggregates had the greatest adsorption potential. This was mainly due to the high surface areas and negative charges associated with fine particles, particularly for several types of clay minerals and organic matter (Huang et al., 2014). In the Freundlich theory, the value of n reflects the heterogeneity or adsorption reaction intensity of the adsorbent; the greater the n value, the

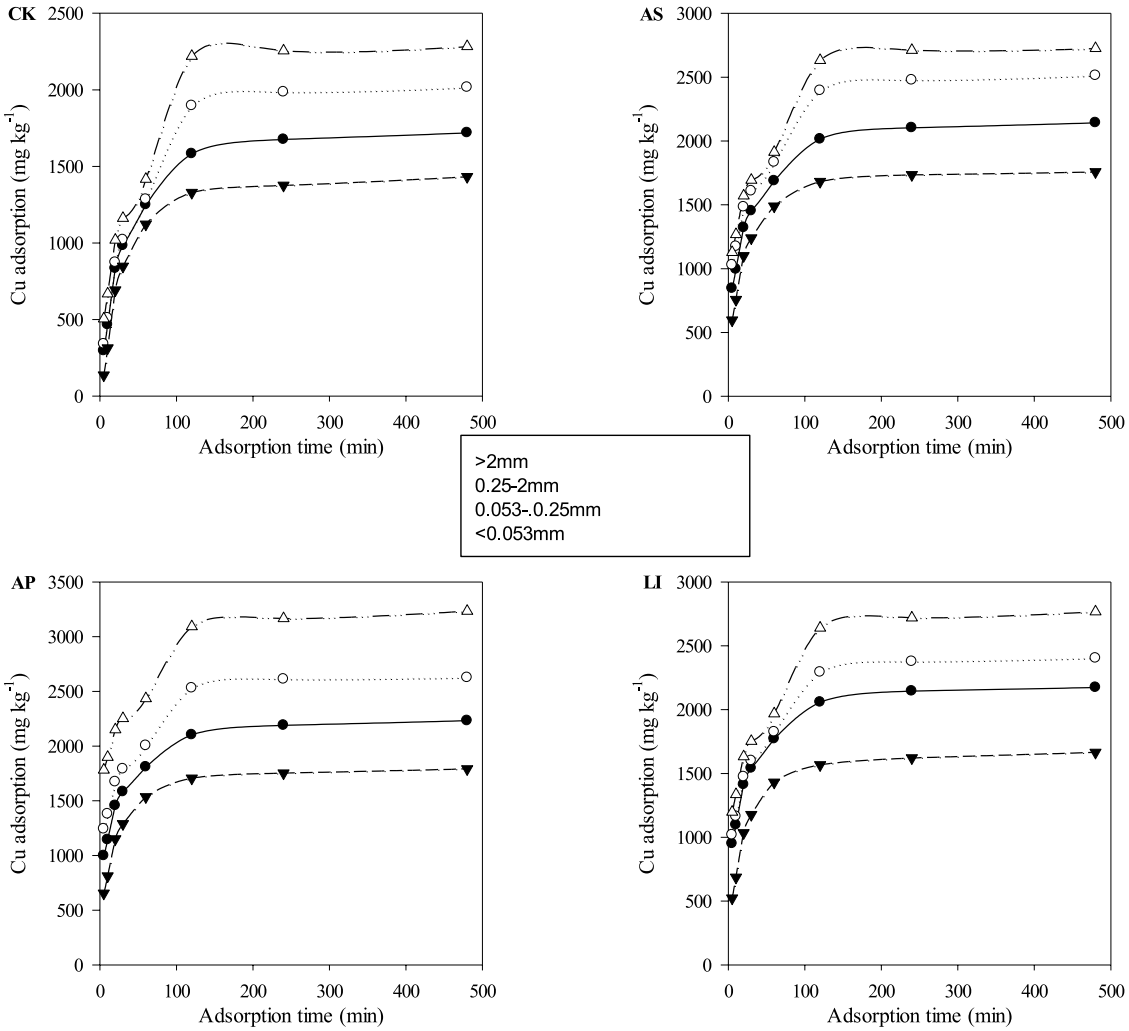

FIGURE 3 | Adsorption kinetics of Cu onto soil aggregates. Experimental data are reported as points and pseudo-second order model data by curves. CK = untreated soil, AS = soda residue + *Elsholtzia splendens*, AP = apatite + *Elsholtzia splendens*, LI = lime + *Elsholtzia splendens*.

better the adsorption performance of the adsorbent (Xie et al., 2021). Compared with CK, the value of n increased after combined remediation in all aggregate size fractions, and the largest increase range was that of AP, followed by LI and AS. This indicates that the adsorption capacity of the soil aggregates improved after combined remediation, which would fix Cu in the soil due to atmospheric deposition and runoff, thereby increasing the total amount of Cu in the soil, which was in good agreement with the experimental data. In rural areas, the impact of this phenomenon is not obvious; however, this phenomenon will increase the total amounts of heavy metals in remediated soil in high settlement areas, resulting in increased risks of contamination.

3.4 Adsorption Kinetics

The results of the kinetic experiments are shown in **Figure 3**; the adsorption amounts increased remarkably during the first 120 min, which accounted for over 92% of the Cu (on average) of the total amount of metals adsorbed within 4 h. Subsequently, the adsorption rate decreased gradually until adsorption equilibrium was reached. The reason for this phenomenon may be that there are sufficient adsorption sites on the aggregate particle surfaces during the initial stage of adsorption to adsorb copper ions in the solution. As the adsorption process progresses, adsorption sites on the aggregate surfaces are gradually occupied, and the number of adsorbed sites is reduced, resulting in a significant decline in the adsorption rate, and finally reaching equilibrium (Apea and Ephraim, 2012). The parameters simulated by the kinetic model are shown in **Table 4**. From the R^2 values, the fitting effect of the pseudo-second-order kinetic equation ($0.995 \leq R^2 \leq 1.00$) was better than that of the pseudo-first-order kinetic equation ($0.579 \leq R^2 \leq 0.978$). The pseudo-second order kinetic equation indicates that the adsorption process is a multi-step reaction, including physical diffusion and chemical

TABLE 4 | Pseudo-first and pseudo-second-order model parameters.

Treatment	Particle size (mm)	Pesudo first-order equation			Pesudo second-order equation			
		Qe (mg g-1)	k1 (min-1)	R2	Qe (mg g-1)	k_2 (g mg^{-1} min^{-1})	v_0 (mg g^{-1} min^{-1})	R^2
CK	>2	1.24	0.0150	0.963	1.82	0.0222	0.0735	0.999
	0.25–2	1.69	0.0180	0.967	2.16	0.0157	0.0733	0.997
	0.053–0.25	0.962	0.0130	0.881	1.54	0.0212	0.0503	0.995
	<0.053	1.86	0.0190	0.898	2.43	0.0156	0.0921	0.996
AS	>2	2.69	0.00500	0.683	2.20	0.0354	0.171	1.00
	0.25–2	3.34	0.00600	0.755	2.60	0.0268	0.181	0.999
	0.053–0.25	2.67	0.00400	0.579	1.81	0.0462	0.151	1.00
	<0.053	3.96	0.00700	0.761	2.82	0.0236	0.188	0.998
AP	>2	1.07	0.0140	0.962	2.28	0.0398	0.207	1.00
	0.25–2	1.51	0.0200	0.983	2.70	0.0321	0.234	0.999
	0.053–0.25	0.855	0.0150	0.905	1.83	0.0490	0.164	1.00
	<0.053	1.48	0.0140	0.921	3.30	0.0280	0.305	0.999
LI	>2	1.10	0.0160	0.978	2.23	0.0409	0.203	1.00
	0.25–2	1.37	0.0170	0.974	2.48	0.0312	0.192	0.999
	0.053–0.25	0.827	0.0140	0.890	1.71	0.0460	0.135	1.00
	<0.053	1.62	0.0160	0.940	2.86	0.0240	0.196	0.998

R-squared values and initial sorption rates calculated from the kinetics experimental data for Cu. CK = untreated soil, AS = soda residue + Elsholtzia splendens, *AP = apatite* + Elsholtzia splendens, *LI = lime* + Elsholtzia splendens.

adsorption processes. The adsorption rate at the chemical adsorption site was the main controlling factor, and the adsorption mechanism was complex (Justi et al., 2004). The adsorption rate constant k_2 fitted by the pseudo-second-order kinetic equation can reflect the speed of the adsorption process. The larger the kinetic rate constant, the faster the adsorption process and the shorter the time required to reach equilibrium. Compared with CK, combined remediation improved the k_2 value in the pseudo-second-order kinetic model for all four particle size aggregates (**Table 3**). This indicates that not only is the maximum adsorption capacity of each aggregate particle size was improved after combined remediation. In addition, the Cu adsorption rate was enhanced. The initial Cu sorption rates (v_0) (0.135–0.305 mg g^{-1} min^{-1}) in the combined remediation were much higher than those of CK (0.0503–0.0921 mg g^{-1} min^{-1}), and the clay-size fraction (<0.053 mm) had the highest v_0 value for Cu compared with the other fractions, except for LI. As a whole, the v_0 increased with decreased particle size, except for the 0.053–0.25 mm fraction. This indicates that the size of the soil particles is not the only factor affecting the initial adsorption rate. The initial adsorption rate is affected by other factors, including soil physical and chemical properties, which are the result of the influence of the comprehensive properties of the soil. The fastest adsorption rate observed in the <0.053 mm fraction might be due to the maximum adsorption capacity and largest specific surface area in the <0.053 mm aggregate fraction.

3.5 Effects of Initial pH on the Adsorption and Desorption

pH is an important factor that affects the adsorption of heavy metal ions onto the soil, which has been accepted by most researchers. Based on the pH influence curve, the copper adsorption by aggregates (**Figure 4**) indicates that the adsorption Cu^{2+} onto aggregates was strongly pH-dependent. The reason for this trend, as discussed in other similar studies (Bradl, 2004), can be explained as follows: when the pH value is low, the metal cations are in competition with the available abundant H^+ for permanently charged sites. Thus, the adsorption of heavy metal cations onto soil is limited; at high pH values, this competition is weak, thereby allowing more metal to be adsorbed. Therefore, under low pH conditions, it is favourable for Cu to be released from the soil to the solution, thereby increasing their migration risk to surface water and groundwater through runoff and leaching. The <0.053 mm size fraction exhibited the highest adsorption among the four different fractions in the experimental pH range. This is consistent with the adsorption kinetics and isotherm results, which indicate that the <0.053 mm fraction had the largest Cu^{2+} adsorption capacity. Some researchers have postulated that the activity of the organic matter and mineral types play major roles in metal enrichment and contribute to a relatively higher portion of specific adsorption in the fine fraction (Acosta et al., 2009). For the different remediation treatments, the adsorption capacity of the aggregates treated with AP for Cu^{2+} was the largest capacity among the different pH values, which indicates that apatite treatment could improve the adsorption capacity of aggregates for Cu^{2+}. It is worth noting that, when the soil had a low pH (pH = 2), only the AP treatment produced a positive adsorption capacity for Cu^{2+}, mainly because the total soil Cu content was high in this area. When the pH of the system was very low, the Cu^{2+} in the aggregates could be dissolved and enter groundwater, which increases the Cu^{2+} concentration in the solution. As the aggregates treated with AP had a strong adsorption capacity for Cu^{2+}, the amount of Cu^{2+} dissolved in the solution was less than the amount of Cu^{2+} adsorbed by the aggregates at a pH of 2; however,

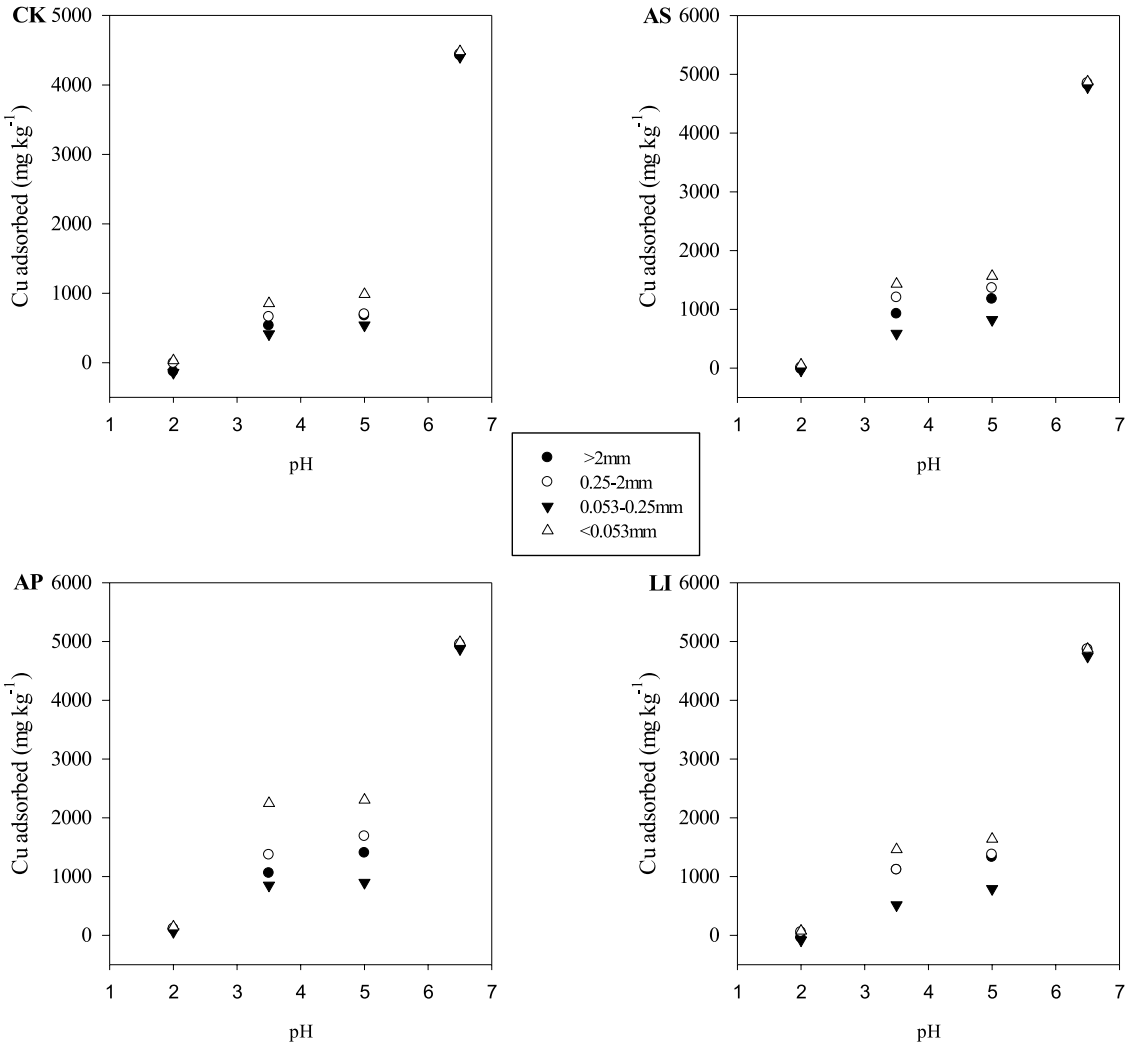

FIGURE 4 | Cu adsorption at different initial pH values. CK = untreated soil, AS = soda residue + *Elsholtzia splendens*, AP = apatite + *Elsholtzia splendens*, LI = lime + *Elsholtzia splendens*.

in other treatments, the amount of Cu^{2+} dissolved in the solution was larger than that adsorbed by the aggregates.

In the desorption experiments using 0.01 mol L^{-1} $NaNO_3$, the Cu^{2+} desorption rate decreased as the initial pH increased (**Table 5**). The desorption rate (%) was very low when the pH exceeded 3.5, and no obvious desorption phenomenon was observed for any fraction at an initial pH of 6.5. Increasing the pH results in more OH–binding Cu^{2+}; therefore, Cu^{2+} desorption becomes more difficult (Dong et al., 2007; Wang et al., 2017) and pH has a dramatic effect on the desorption of Cu^{2+}. The desorption rate of the <0.053 mm fraction was the lowest, which was mainly related to the large adsorption capacity of the fine particle size aggregates. For the different treatments, all of the particle size fractions treated with AP had the lowest desorption rates at all four pH values, which may also be due to the large adsorption capacity of apatite-treated aggregates for Cu^{2+}. In a previous study, we found that the total Cu in the amended soils was higher than that of the untreated soil. We speculated that this may be attributed to more heavy metals immobilised in the 0—0.17 m depth (topsoil) of amendment-treated soils than those in the untreated soil (Cui et al., 2014). The results of this study further confirm that more Cu was retained and immobilised in the soils with the application of amendments, especially apatite, resulting in higher Cu concentrations in the amended soils than in the untreated soil (*Soil Characteristics and Plant Biomass* Section). Moreover, the results also indicate that apatite had the lowest Cu leaching risk among the amendments.

4 CONCLUSION

With the addition of soda residue, apatite, and lime, the Cu concentrations in the $CaCl_2$ extractable and exchangeable fractions significantly decreased, while the concentrations of SOC increased significantly. The highest heavy metal concentrations were observed in the smallest aggregates

TABLE 5 | Cu^{2+} Desorption rate (%) at different initial pH values.

Treatment	2.0					3.5					5.0					6.5				
	>2 mm	0.25–2 mm	0.053—0.25 mm	<0.053 mm	>2 mm	0.25–2 mm	0.053–0.25 mm	<0.053 mm	>2 mm	0.25–2 mm	0.053–0.25 mm	<0.053 mm	>2 mm	0.25–2 mm	0.053–0.25 mm	<0.053 mm	>2 mm	0.25–2 mm	0.053–0.25 mm	<0.053 mm
CK	–82.7	-1.04×10^3	–40.6	323	57.8	52.7	61.7	47.5	51.4	52.7	52.6	43.8	6.17	6.20	5.62	6.34				
AS	–515	1.30×10^3	–184	224	41.6	34.5	54.4	31.2	33.7	30.6	41.4	28.3	3.17	2.78	4.16	2.44				
AP	101	98.7	139	155	37.4	37.7	34.1	15.5	25.8	25.0	37.0	15.8	2.16	1.73	3.21	1.26				
LI	–263	256	–132	225	34.0	35.0	54.4	31.8	30.4	31.9	44.0	29.9	2.44	2.79	4.05	2.47				

(<0.053 mm), and the Cu concentrations in both the >2 mm and 0.25–2 mm size fractions followed the order of soda residue > apatite > lime > control, while the Cu concentrations in both the 0.053–0.25 mm and <0.053 mm size fractions followed a descending order of apatite > soda > residue > lime > control. The highest mass loading of Cu was observed in the 0.25–2 mm size fraction, followed by the 0.053–0.25 mm, > 2 mm, and <0.053 mm size fractions, respectively. The Freundlich equation was more accurate than the Langmuir equation for fitting the adsorption characteristics under different initial metal concentrations in the isotherm adsorption experiments. In the kinetic adsorption experiments, the adsorption data were successfully fitted using a pseudo-second order model for Cu, and the initial sorption rates (v_0) of Cu in the combined remediation were much higher than those of CK, and v_0 increased with a decrease in particle size, except for the 0.053–0.25 mm fraction. The amount of Cu adsorbed increased as the pH increased. After being introduced to the soil, water-soluble Cu was more likely to be enriched in the clay-size aggregates, and the fine soil particles are also the final metal transporters. The Cu^{2+} desorption rate decreased as the initial pH increased, and for different particle sizes fractions, the desorption rate of the <0.053 mm fraction was the lowest. For different treatments, all of the particle size aggregates treated with AP had the lowest desorption rates at all pH values. *In situ* remediation can therefore improve Cu adsorption onto each aggregate particle size fraction, thereby reducing desorption. When no new heavy metals enter the soil, the risk of heavy metal migration in the soil is reduced. However, in an area where the pollution source is still present, an increase in the total Cu concentration in the soil may occur, thereby increasing the associated environmental risk.

DATA AVAILABILITY STATEMENT

The raw data supporting the conclusions of this article will be made available by the authors, without undue reservation.

AUTHOR CONTRIBUTIONS

LX is responsible for the writing of the paper and the conduct of the experiment, XX has made contributions to the revision of the language of the paper, JP and MJ share their ideas and logic modification of the paper.

FUNDING

The research was funded by the Key Scientific Research Projects of Henan Province Colleges and Universities (22B180010), The Scientific and Technological Research Projects in Henan Province (222102320317), the PhD Special Project of Nanyang Normal University (2018ZX018), the Scientific and Technological Research Projects in Henan Province (212102310844).

REFERENCES

Acosta, J. A., Cano, A. F., Arocena, J. M., Debela, F., and Martínez-Martínez, S. (2009). Distribution of Metals in Soil Particle Size Fractions and its Implication to Risk Assessment of Playgrounds in Murcia City (Spain) [J]. *Geoderma* 149 (1–2), 101–109. doi:10.1016/j.geoderma.2008.11.034

Alireza, E., and Fahadani (2018). Experimental Study of the Effect of Material and Arrangement of Electrodes and Voltage on the Electro-Remediation of Saturated Clays Containing Chloride and Sulfate Ions [J]. *Arabian J. Geosciences* 11 (21), 671–682.

Apea, O. B., and Ephraim, J. H. (2012). EFFECT OF HUMIC ACID ON THE KINETICS AND MECHANISM OF COPPER ADSORPTION IN SOIL-SOLUTION SYSTEM [J]. *J. Appl. Sci. Environ. Sanitation* 7 (2), 137–146.

Bradl, H. B. (2004). Adsorption of Heavy Metal Ions on Soils and Soils Constituents. *J. Colloid Interf. Sci.* 277 (1), 1–18. doi:10.1016/j.jcis.2004.04.005

Brahim, K., Soussi-Baatout, A., and Khattech, I. (2017). Dissolution Kinetics of Fluorapatite in the Hydrochloric Acid Solution [J]. *J. Therm. Anal. Calorim.* 129 (7), 1–8. doi:10.1007/s10973-017-6221-8

Cui, H., Fan, Y., Xu, L., Zhou, J., Zhou, D., Mao, J., et al. (2016). Sustainability of *In Situ* Remediation of Cu- and Cd-Contaminated Soils with One-Time Application of Amendments in Guixi, China. *J. Soils Sediments* 16 (5), 1498–1508. doi:10.1007/s11368-015-1317-x

Cui, H., Zhou, J., Si, Y., Mao, J., Zhao, Q., Fang, G., et al. (2014). Immobilization of Cu and Cd in a Contaminated Soil: One- and Four-Year Field Effects. *J. Soils Sediments* 14 (8), 1397–1406. doi:10.1007/s11368-014-0882-8

Derakhshan Nejad, Z., Rezania, S., Jung, M. C., Al-Ghamdi, A. A., Mustafa, A. E.-Z. M. A., and Elshikh, M. S. (2021). Effects of fine Fractions of Soil Organic, Semi-organic, and Inorganic Amendments on the Mitigation of Heavy Metal(loid)s Leaching and Bioavailability in a post-mining Area. *Chemosphere* 271 (3), 129538–129549. doi:10.1016/j.chemosphere.2021.129538

Deshpande, T. L., Ballal, D. K., and Kalamkar, R. J. (1958). Effect of Growing Cotton Continuously and in Rotation with Different Crops on the Fertility of Black Cotton Soil. *Proc. Indian Acad. Sci. - Section B* 47 (2), 102–113. doi:10.1007/bf03051038

Dong, C. X., Li, L. Q., and Wang, F. (2007). Sorption-desorption of Cu^{2+} by Paddy Soil and the pH Change of Equilibrium Solution [J]. *J. Agro-Environment Sci.* 2, 521–525. doi:10.3321/j.issn:1672-2043.2007.02.022

Hardie, M., Clothier, B., and Bound, S. (2014). Does Biochar Influence Soil Physical Properties and Soil Water Availability? [J]. *Plant and Soil* 376 (1-2), 347–361. doi:10.1007/s11104-013-1980-x

Haynes, R. J., and Graham, M. H. (2004). Soil Biology and Biochemistry - a New Direction for South African Soil Science? *South Afr. J. Plant Soil* 21 (5), 330–344. doi:10.1080/02571862.2004.10635068

He, G., Zhang, Z., Wu, X., Cui, M., Zhang, J., and Huang, X. (2020). Adsorption of Heavy Metals on Soil Collected from Lixisol of Typical Karst Areas in the Presence of CaCO3 and Soil Clay and Their Competition Behavior. *Sustainability* 12 (18), 7315–7334. doi:10.3390/su12187315

Ho, Y., and Mckay, G. (2000). The Kinetics of Sorption of Divalent Metal Ions onto Sphagnum moss Peat. *Water Res.* 34 (3), 735–742. doi:10.1016/s0043-1354(99)00232-8

Huang, B., Yuan, Z., Li, D., Zheng, M., Nie, X., and Liao, Y. (2020). Effects of Soil Particle Size on the Adsorption, Distribution, and Migration Behaviors of Heavy Metal(loid)s in Soil: a Review. *Environ. Sci. Process. Impacts* 22 (4), 1596–1615. doi:10.1039/d0em00189a

Huang, B., Li, Z., Huang, J., Guo, L., Nie, X., Wang, Y., et al. (2014). Adsorption Characteristics of Cu and Zn onto Various Size Fractions of Aggregates from Red Paddy Soil. *J. Hazard. Mater.* 264 (15), 176–183. doi:10.1016/j.jhazmat.2013.10.074

Huang, B., Li, Z., Li, D., Yuan, Z., Chen, Z., and Huang, J. (2017). Distribution Characteristics of Heavy Metal(loid)s in Aggregates of Different Size Fractions along Contaminated Paddy Soil Profile. *Environ. Sci. Pollut. Res.* 24, 23939–23952. doi:10.1007/s11356-017-0012-4

Justi, K. C., Laranjeira, M. C. M., Neves, A., Mangrich, A. S., and Fávere, V. T. (2004). Chitosan Functionalized with 2[-bis-(pyridylmethyl) Aminomethyl]4-Methyl-6-Formyl-Phenol: Equilibrium and Kinetics of Copper (II) Adsorption. *Polymer* 45 (18), 6285–6290. doi:10.1016/j.polymer.2004.07.009

Kwak, J. I., Nam, S. H., Kim, S. W., Bajagain, R., Jeong, S. W., and An, Y. J. (2019). Changes in Soil Properties after Remediation Influence the Performance and Survival of Soil Algae and Earthworm. *Ecotoxicol Environ. Saf.* 174, 189–196. doi:10.1016/j.ecoenv.2019.02.079

Li, J., Jia, C., Lu, Y., Tang, S., and Shim, H. (2015). Multivariate Analysis of Heavy Metal Leaching from Urban Soils Following Simulated Acid Rain. *Microchemical J.* 122 (9), 89–95. doi:10.1016/j.microc.2015.04.015

Li, P., Wang, X. X., and Zhang, T. L. (2009). Distribution and Accumulation of Copper and Cadmium in Soil–Rice System as Affected by Soil Amendments [J]. *Water Air Soil Pollut.* 196 (1-4), 29–40. doi:10.1007/s11270-008-9755-3

Li, Y., Deng, M., Wang, X., Wang, Y., Li, J., Xia, S., et al. (2021). In-situ Remediation of Oxytetracycline and Cr(VI) Co-contaminated Soil and Groundwater by Using Blast Furnace Slag-Supported Nanosized Fe0/FeSx. *Chem. Eng. J.* 412 (5), 128706–128715. doi:10.1016/j.cej.2021.128706

Li, Z., Zhao, B., Hao, X., and Zhang, J. (2017). Effects of Residue Incorporation and Plant Growth on Soil Labile Organic Carbon and Microbial Function and Community Composition under Two Soil Moisture Levels. *Environ. Sci. Pollut. Res. Int.* 24, 18849–18859. doi:10.1007/s11356-017-9529-9

Lo, A., Nguyen, X. T., and Hankins,] N. P. (2016). Recovery of Heavy Metal Ions and Recycle of Removal Agent in the Polymer–Surfactant Aggregate Process [J]. *Separat. Purif. Technol.* 159 (8), 169–176.

Ma, J., and Singhirunnusorn, W. (2012). Distribution and Health Risk Assessment of Heavy Metals in Surface Dusts of Maha Sarakham Municipality. *Proced. - Soc. Behav. Sci.* 50 (1), 280–293. doi:10.1016/j.sbspro.2012.08.034

Madej, N. P., Rezdemora, P. A., and Burgos, P. (2010). Do amended, Polluted Soils Require Re-treatment for Sustainable Risk Reduction? Evidence from Field Experiments [J]. *Geoderma* 159 (1), 174–181. doi:10.1016/j.geoderma.2010.07.009

Mariela, A., and Fernandez (2015). Sorption of Zn(II) and Cu(II) by Four Argentinean Soils as Affected by pH, Oxides, Organic Matter and clay Content [J]. *Environ. Earth Sci.* 74 (5), 4201–4214.

Mobasherpour, I., Salahi, E., and Ebrahimi, M. (2014). Thermodynamics and Kinetics of Adsorption of Cu(II) from Aqueous Solutions Onto Multi-Walled Carbon Nanotubes [J]. *J. Saudi. Chem. Soc.* 18, 792–801. doi:10.1016/j.jscs.2011.09.006

Oliva, J., Cama, J., Cortina, J. L., Ayora, C., and De Pablo, J. (2012). Biogenic Hydroxyapatite (Apatite II) Dissolution Kinetics and Metal Removal from Acid Mine Drainage. *J. Hazard. Mater.* 213-214, 7–18. doi:10.1016/j.jhazmat.2012.01.027

Page, A. L. (1992). Methods of Soil Analysis. Part 2. Chemical and Microbiological Properties [J]Wi. *Am. Soc. Agron. Inc Soil Sci. Soc. America Inc.*

Pansu, M., and Gautheyrou, J. (2006). Handbook of Soil Analysis. Mineralogical, Organic and Inorganic Methods [J]. *Int. J. Cancer* 115 (1), 36–45.

Pez-Bellido, R. J. L., Lal, R., and Danneberger, T. K. (2010). Plant Growth Regulator and Nitrogen Fertilizer Effects on Soil Organic Carbon Sequestration in Creeping Bentgrass Fairway Turf [J]. *Plant & Soil* 332 (1-2), 247–255. doi:10.1007/s11104-010-0289-2

Samsuri, A. W., Fahmi, A. H., Jol, H., and Daljit, S. (2019). Particle Size and Rate of Biochar Affected the Phytoavailability of Cd and Pb by Mustard Plants Grown in Contaminated Soils. *Int. J. Phytoremediation* 22 (6), 567–577. doi:10.1080/15226514.2019.1687423

Shaver, T. M., Peterson, G. A., and Sherrod, L. A. (2003). Cropping Intensification in Dryland Systems Improves Soil Physical Properties: Regression Relations [J]. *Geoderma* 116 (1–2), 149–164. doi:10.1016/s0016-7061(03)00099-5

Tao, M. J., Zhou, J., and Liang, J. N. (2014). Study on Atmospheric Deposition Characteristics of Cu and Cd in Summer Around One Smelting Factory [J]. *Environ. Monit. China* 30 (6), 108–113.

Wang, Z., Cao, M., and Cai, W., The Effect of Humic Acid and Fulvic Acid on Adsorption-Desorption Behavior of Copper and Zinc in the Yellow Soil. 11th Asian Conference on Chemical Sensors:(ACCS2015), Changsha, Hunan, China (Chemical Sensors), 2017.

Xiao, R., Zhang, M., and Yao, X. (2016). Heavy Metal Distribution in Different Soil Aggregate Size Classes from Restored Brackish Marsh, Oil Exploitation Zone, and Tidal Mud Flat of the Yellow River Delta [J]. *J. Soils Sediments* 16 (3), 1–10. doi:10.1007/s11368-015-1274-4

Xie, G., Li, B., Tang, L., Rao, L., and Dong, Z. (2021). Adsorption-desorption and Leaching Behaviors of Broflanilide in Four Texturally Different Agricultural

Soils from China. *J. Soils Sediments* 21 (2), 724–735. doi:10.1007/s11368-020-02831-9

Xu, G., Li, Z., and Li, P. (2013a). Fractal Features of Soil Particle-Size Distribution and Total Soil Nitrogen Distribution in a Typical Watershed in the Source Area of the Middle Dan River, China. *Catena* 101 (2), 17–23. doi:10.1016/j.catena.2012.09.013

Xu, G., Liu, M., and Li, G. (2013b). Stabilization of Heavy Metals in Lightweight Aggregate Made from Sewage Sludge and River Sediment. *J. Hazard. Mater.* 260 (1), 74–81. doi:10.1016/j.jhazmat.2013.04.006

Xu, L., Yu, C., Mao, Y., Zong, Y., Zhang, B., Chu, H., et al. (2020). Can Flow-Electrode Capacitive Deionization Become a New In-Situ Soil Remediation Technology for Heavy Metal Removal? *J. Hazard. Mater.* 402, 123568–123578. doi:10.1016/j.jhazmat.2020.123568

Xu, L., Cui, H., Zheng, X., Zhou, J., Zhang, W., Liang, J., et al. (2017). Changes in the Heavy Metal Distributions in Whole Soil and Aggregates Affected by the Application of Alkaline Materials and Phytoremediation. *RSC Adv.* 7 (65), 41033–41042. doi:10.1039/c7ra05670b

Xue, Z.-J., Liu, S.-Q., Liu, Y.-L., and Yan, Y.-L. (2012). Health Risk Assessment of Heavy Metals for Edible Parts of Vegetables Grown in Sewage-Irrigated Soils in Suburbs of Baoding City, China. *Environ. Monit. Assess.* 184 (6), 3503–3513. doi:10.1007/s10661-011-2204-6

Yu, H., Zhang, W. B., and Yu, J. P. (2011). Distribution and Potential Ecological Risk Assessment of Heavy Metals in Surface Sediments of Hongze Lake. *Huan Jing Ke Xue* 32 (2), 437–444.

Zhang, Z., Abuduwaili, J., and Jiang, F. (2015). Heavy Metal Contamination, Sources, and Pollution Assessment of Surface Water in the Tianshan Mountains of China [J]. *Environ. Monit. Assess.* 187 (2), 4191–4204.

Zhang, Z., Wu, X., Tu, C., Huang, X., Zhang, J., Fang, H., et al. (2020). Relationships between Soil Properties and the Accumulation of Heavy Metals in Different Brassica Campestris L. Growth Stages in a Karst Mountainous Area. *Ecotoxicology Environ. Saf.* 206, 111150–111159. doi:10.1016/j.ecoenv.2020.111150

Zhao, J., Chen, S., Hu, R., and Li, Y. (2017). Aggregate Stability and Size Distribution of Red Soils under Different Land Uses Integrally Regulated by Soil Organic Matter, and Iron and Aluminum Oxides. *Soil Tillage Res.* 167, 73–79. doi:10.1016/j.still.2016.11.007

Zheng, R.-L., Cai, C., Liang, J.-H., Huang, Q., Chen, Z., Huang, Y.-Z., et al. (2012). The Effects of Biochars from rice Residue on the Formation of Iron Plaque and the Accumulation of Cd, Zn, Pb, as in rice (Oryza Sativa L.) Seedlings. *Chemosphere* 89 (7), 856–862. doi:10.1016/j.chemosphere.2012.05.008

Zhou, J., Liang, J., Hu, Y., Zhang, W., Liu, H., You, L., et al. (2018). Exposure Risk of Local Residents to Copper Near the Largest Flash Copper Smelter in China. *Sci. Total Environ.* 630, 453–461. doi:10.1016/j.scitotenv.2018.02.211

Zhu, Q., de Vries, W., Liu, X., Hao, T., Zeng, M., Shen, J., et al. (2018). Enhanced Acidification in Chinese Croplands as Derived from Element Budgets in the Period 1980-2010. *Sci. Total Environ.* 618, 1497–1505. doi:10.1016/j.scitotenv.2017.09.289

Conflict of Interest: The authors declare that the research was conducted in the absence of any commercial or financial relationships that could be construed as a potential conflict of interest.

Publisher's Note: All claims expressed in this article are solely those of the authors and do not necessarily represent those of their affiliated organizations, or those of the publisher, the editors and the reviewers. Any product that may be evaluated in this article, orclaim that may be made by its manufacturer, is not guaranteed or endorsed by the publisher.